INTERNATIONAL JOURNAL OF SCIENCE AND NATURE

www.scienceandnature.org

SYNTHESIS AND PHYSICAL PROPERTIES OF THE NEW DOUBLE PEROVSKITE X_2AlVO_6 (X=Ca, Sr & Ba)

[1,2]Yousef A. Alsabah, [1,*]Abdelrahman A. Elbadawi, [1]Mohamed A. Siddig, [1,3]Mohammad I. Mohammed
[1]Department of Physics, Faculty of Science and Technology, Al Neelain University, Khartoum, Sudan
[2]Department of Physics, Faculty education and applied Science, Hajjah University, Hajjah, Yemen
[3]Department of Physics, Faculty education, Nile Valley University, Attbra, Sudan
Correspondence author email: bahlaoy@yahoo.com

ABSTRACT
Three members of the double perovskite materials X_2AlVO_6 (X = Ca, Sr and Ba) were synthesis by solid state interaction method. Crystal structure, optical and dielectrical properties calculations of these double perovskite materials were described. X- Ray Diffraction (XRD), Fourier Transform Infra Red (FTIR), Ultra Violet visible (UV), and Impeadence spectroscopies were used as analytical techniques. XRD measurements showed that these materials are crystallize in orthorhombic double perovskite structures with (Pnma) space group. Unit cell parameters, atomic positions, crystalline size and site occupancies were calculated by standared Rietveld method through the Fullprof program. Lattice parameters were a=b= 5.4798 Å and c = 7.7621 Å for Ca_2AlVO_6, a = b = 5.5518 Å and c = 7.8695Å for Sr_2AlVO_6 and a =b = 5.5759 Å and c = 7.89380 Å for Ba_2AlVO_6. The energy gap were calculated for Ca_2AlVO_6, Sr_2AlVO_6 and Ba_2AlVO_6, and found to be 4.16eV, 4.79eV and 4.87eV respectivily.

KEY WORDS: Double perovskite, energy gap, Impedance, space group, XRD.

INTRODUCTION

In the recent past, a high attention was focus on perovskite type compounds which show a large diversity of interesting electrical, optical and magnetic functional properties outcome their compositional and structural variety. As a the privious studies, many compounds that belong to this group have been synthesized. The perovskites formula is ABO_3, where A and B might be almost any metal or semimetal from the periodic table [1-3]. The general chemical formula of double perovskite oxides expressed as $A_2BB`O_6$, where A is Ca, Sr and Ba. The B site is ocuppied by first row of 3d magnetic element in the perodic table, where the B` site is ocuppied by the 4d non-magnetic elements, with O atom located in between forming alternate BO_6 octahedral and B-O-B bonds, The wide range of double perovskite material is due to alteration at the magnetic and non –magnetic of B and B` elements as well as the A-site cations [4, 5]. In particular, the compositions A_2BMoO_6, where B = Fe, Mn, Cr are magnetic ions are currently studied for their potentiality as magnetoresistive systems and thermoelectrics[6]. The synthesis and structural properties of new Dy_2MgTiO_6 and Gd_2MgTiO_6 perovskite-like material was performed. These materials crystallize in monoclinic double perovskites with $P2_1/n$ space group that showed by Rietveld analyses. These double perovskite compounds had semiconducting behavior, which showed by Density of states results, with energy gap between 0.6 eV and 0.73 eV and effective magnetic moment of 13.9 μ_B and 10.1 μ_B for Dy_2MgTiO_6 and Gd_2MgTiO_6, consecutively, which are majority due to the f-orbitals of the rare earth cations [7]. $ALaFeTiO_6$ (A= Ba, Sr and Ca) double perovskite oxides of chemical mode had been done by following the precursor method, and the structural analysis of $BaLaFeTiO_6$ is cubic and consistency with it's tolerance factor [8]. $La_{1-x}K_xMnO_3$ perovskites (x = 0.1, 0.125 and 0.150) had prepared by solid-state reaction method, rhombohedrally-distorted structure showed by the Rietveld refinements of X-ray diffraction patterns [9]. Spin-reorientation situation of $YFe_{1-x}Mn_xO_3$ (x = 0.0, 0.2) perovskite had showed and corroborated by magnetic properties and Mossbauer spectroscopy. The spin-reorientation transition temperature (TSR) increment when the N´eel temperature (TN) decrement with increasing x, under the weakening of the exchange interaction between Fe ions. They shown occurrence of spin- reorientation relative to crystal axes from the Mossbauer spectra of $YFe_{1-x}Mn_xO_3$ (x = 0.1, 0.2) [10].

Solid-state technique was used to synthesized Ca_2CeNbO_6 double perovskite oxide. The orthorhombic perovskite structure, the electrical and optical properties of this materail had studied, all the peak that refer to the double perovskite structure bonds showed in small hump. The frequency- dependent electrical data were analyzed in the framework of conductivity and electric modulus formalisms. Frequency dependent imaginary electric modulus (M``) subjected to an Arrhenius law[11]. The $Sr_2CaW_xMo_{1-x}O_6$ double perovskite series have been synthesized by solid–state reaction. The self- activated host material emit strong blue lights at round 435 and 468 nm upon the excitation of near –UV at about 290nm due to W-O charge transfer transition. The hosts show weak orange–red emission by excitation of 400nm due to Mo-charge transfer transtion[12]. The aim of this work is to synthesizse new samples of double provskite oxides by solid state interaction method. In addition, the structural, optical and

electrical properties of the new double peroviskite X_2AlVO_6 Where (X=Ca, Sr and Ba) is invistigated.

MATERIALS & METHODS

The new samples of double provskite oxides synthesized by solid state interaction method by different treatments to get single phase for the samples. The samples prepared by mixing stoichiometric amounts of Al_2O_3, V_2O_5 with ($CaCO_3$, $SrCO_3$ and $BaCO_3$) all from Alfa Acer of purity 99.9% were used to prepare the X_2AlVO_6 Where X are (Ca or Sr or Ba). The mixtures of compounds grinded in agate mortar with the addation of acitone then heated in air, after put in crucibles initially at 800°C during 12 hours four times, pellet in around shape and heated in 1200°C three times permeated every time grinding with the addition of acetone, the ratio of all amounts calculated by the fowling equations:

$$\left.\begin{matrix}2CaCO_3\\2SrCO_3\\2BaCO_3\end{matrix}\right\} + \frac{1}{2}\,Al_2O_2 + \frac{1}{2}\,V_2O_5 \rightarrow X_2AlVO_6 + CO_2\uparrow \qquad (1)$$

X-ray diffraction (XRD) used is a Bruker - axs D8- Focus X-ray diffractometer. The data were collected for the 2θ range 20^o – 80^o at step size of 0.02 and count time of 5s. The collected data are then fed to fullprof suite[13] for determination of the lattice parameters, space group, atom`s positions and crystalline size by scherrer equation[14].

$$D = \frac{0.94\lambda}{\beta_{1/2}\cos\theta} \qquad (2)$$

A Fourier transform infrared (FTIR) spectrum was recorded in transmittance mode at room temperature between 400 and 2000 cm^{-1} with a Fourier transform infrared spectrometer (Satellite FTIR 5000) in the wavelength range of 400 to 4000 cm^{-1} [15]. The UV-visible absorbtion spectrum was obtained by an automatic recording single beam spectrophotometer type UV Mini 1240 manufactured by Shimadzu company–Japan and coming with serial number A10934081718SM. HCl was used as a reference for 100% absorbance, after that the Energy Gap was measured for all samples [16].

The LCR Meter used to study the dielectric properties; both flat surfaces of pellets were electrode with fine silver paint and were kept at 1200°C for 12 h prior to conducting the experiment impedance of the sample measured as a function of frequency (10 Hz- 1MHz) at room temperature. The resistivity, conductivity and dielectric constant were calculated at ω = 100 Hz [17].

RESULTS & DISCUSSION

X-ray diffraction (XRD) analysis

Figure (1) shows the room temperature XRD pattern of Ca_2AlVO_6, Sr_2AlVO_6 and Ba_2AlVO_6 respectively. All reflection peaks of the X-ray profile and lattice parameters determined with full proof program, they had orthorhombic crystal structure with (Pnma) space group. The XRD results have been fitted by standard Rietveld method using the Fullprof suite and Figure (2) shows the case of Ba_2AlVO_6. Elena-Adriana Perianu [1] studied Preparation and Dielectric Spectroscopy Characterization of A_2MnMoO_6 (A = Ca, Sr and Ba) Double Perovskites and they found that the size of cation X seems to be relevant to the structural distortions. In our case the tolerance factor increases with the size of cation X: with increasing of the ionic radius in the series $r_{Ca2+} < r_{Sr2+} < r_{Ba2+,}$ the tolerance factor increases from t = 0.9064 (for compound with Ca) at t = 0.9584 (for compound with Sr) and at t = 1.0160 (for compound with Ba)[1]**.** The size of cation X seems to be relevant to the strucural distorsions. In our case the tolerance factor increases with the size of the cation X : with increasing of the ionic radius in the series $r_{Ca2+} < r_{Sr2+} < r_{Ba2+}$ the tolerance factor $T = (r_A+r_o)/((2)^{1/2}(r_B+r_o))$ [18] increases from T=0.9926 (for compound with Ca) at T= 1.0496 (for compound with Sr) and at T= 1.1127 (for compound with Ba), and the crystalline size increases with the size of the cation X : with increasing of the ionic radius in the series $r_{Ca2+} < r_{Sr2+} < r_{Ba2+}$ the crystalline size increases from D = 61.61nm (for compound with Ca) at D = 69.83nm (for compound with Sr) and at D = 76.38nm (for compound with Ba). The obtained lattice parameters and atoms position listed in Table (1), crystalline size calculated by scherrer equation [19]. Figure (3) show the relation between crystalline size and Tolerance factor with ionic radius of X- site, and the crystalline size and tolerance factor are list in table (2).

(FTIR – UV visible) spectroscopy analysis

The two major absorptions peaks are explicitly split, probably as an effect of the orthorhombic distortion of the unit cell. The strong high-energy band centered at about 640 cm^{-1} can surely be assigned to the anti-symmetric stretching mode of the ($Al–O_6$) and ($V–O_6$) octahedra, due to the higher charge of this cation. Another interesting point appear by this spectra is the presence of the high intensity band at 825 cm^{-1} which can eventually be assigned to the symmetric stretching vibration of these octahedra as explained in figure (4). The positions of these bands suggests relatively long ($Al–O_6$) and ($V–O_6$) bonds [18]. All the peaks in the spectrum are assigned small hump at approximately 1645 cm^{-1} which is due to the presence of adsorbed moisture in KBr during the synthesis of all samples[20]. The peak around 1400 cm^{-1} likely corresponds to overtones of the substantial vibrations in X_2AlVO_6 where X= (Ca, Sr and Ba), Chandrahas Bharti,T.P. Sinha showed that in another study [21]. Figure (5) shows the FTIR spectrum of X_2AlVO_6 where (X= Ca,Sr and Ba). All the peaks in the spectra are the characteristics of the material.

TABLE 1: The lattice parameter and atoms position, of the samples

Element	Coordinate	Ca_2AlVO_6	Sr_2AlVO_6	Ba_2AlVO_6
		Pnma	Pnma	Pnma
$Ca_2/Sr_2/Ba_2$	X	0.50000	0.50000	0.50000
	Y	0.50000	0.50000	0.50000
	Z	0.25000	0.25000	0.25000
Al	X	0.0000	0.0000	0.0000
	Y	0.0000	0.0000	0.0000
	Z	0.0000	0.0000	0.0000
V	X	0.50000	0.50000	0.50000
	Y	0.0000	0.50000	0.0000
	Z	0.0000	0.0000	0.0000
O1	X	0.2504	0.0000	0.25040
	Y	0.24960	0.0000	0.25040
	Z	0.0000	0.26120	0.0000
O2	X	0.0000	0.19040	0.0000
	Y	0.0000	0.33380	0.0000
	Z	0.24960	0.0000	0.24960
$\alpha = \beta = \gamma$		90	90	90
a A^o		5.4798	5.5518	5.5759
b A^o		5.4798	5.5518	5.5759
c A^o		7.76421	7.8695	7.893801

TABLE 2: Tolerance factor and crystalline size (nm) of all samples

Samples	T (Tolerance Factor)	D (Crystalline size)(nm)
Ca_2AlVO_6	0.9064	61.61
Sr_2AlVO_6	0.9584	69.83
Ba_2AlVO_6	1.0160	76.38

TABLE 3: the wave length and band gap energy list of all samples

Samples	(λ)nm	band gap energy (eV)
Ca_2AlVO_6	300	4.1
Sr_2AlVO_6	259	4.7
Ba_2AlVO_6	254	4.8

TABLE 4: Dielectric Impedance parameters (and dielectric constant at ω= 100 Hz) at room temperature

Sample	Z`	Z``	Z∗(MΩ)	$\rho^*(\Omega.m)$	$\sigma^*(\Omega.m)^{-1}$	ε^*
Ca_2AlVO_6	$4.1x10^7$	$5.0x10^8$	1641	$6.24x10^5$	$1.6x10^{-6}$	$1.1x10^{-9}$
Sr_2AlVO_6	$2.1x10^8$	$3.4x10^8$	407	$2.38x10^5$	$4.2x10^{-6}$	$9.3x10^{-9}$
Ba_2AlVO_6	$1.2x10^8$	$2.3x10^8$	123	$1.59x10^5$	$6.3x10^{-6}$	$5.9x10^{-9}$

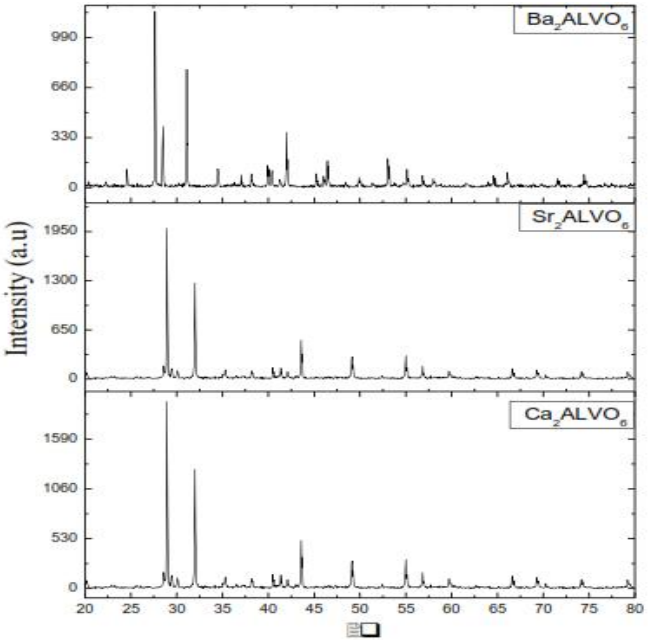

FIGURE 1: The room temperature XRD pattern of Ca_2AlVO_6, Sr_2AlVO_6 and Ba_2AlVO_6 samples

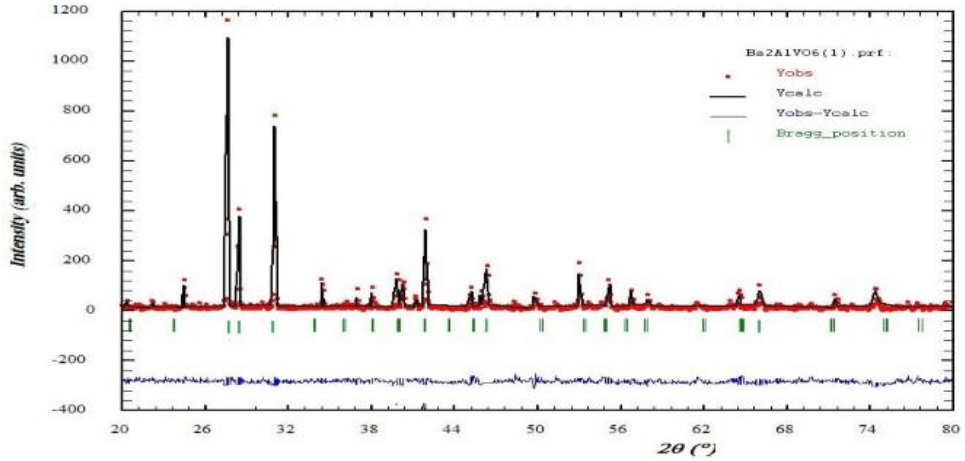

FIGURE 2: The XRD diffractograms of the Ba_2AlVO_6 sample

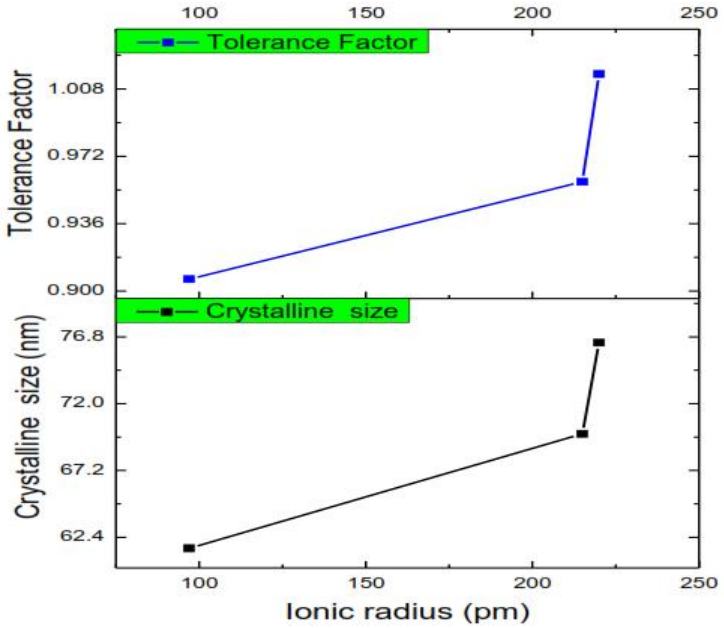

FIGURE 3: Relation between crystalline size and Tolerance Factor ionic with radius of X- site

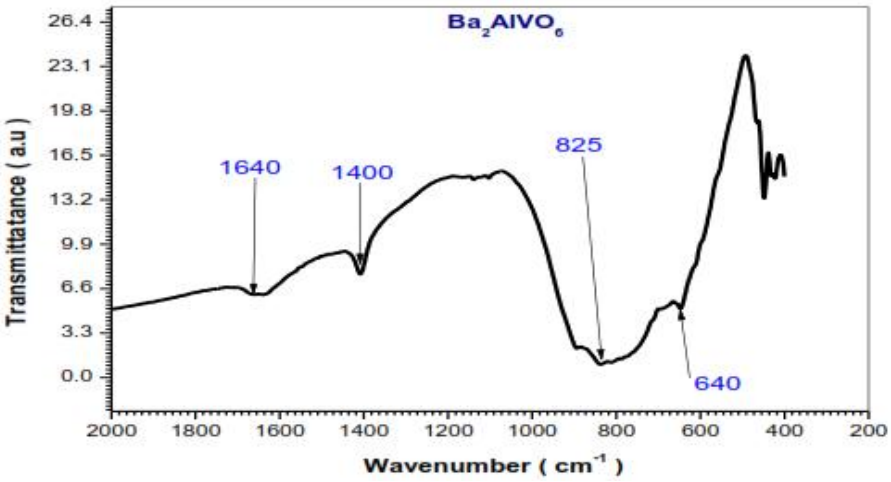

FIGURE 4: The FTIR of the double perovskite Ba_2AlVO_6

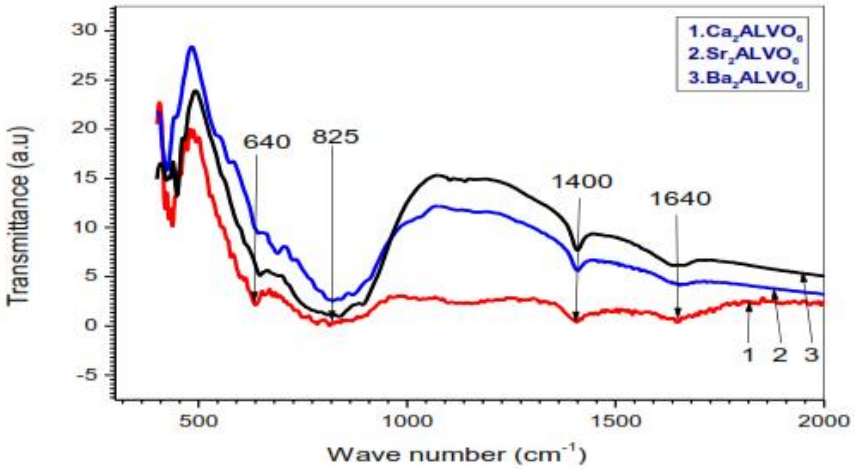

FIGURE 5: The FTIR spectra of Ca_2AlVO_6, Sr_2AlVO_6 and Ba_2AlVO_6 samples

Figure (6) shows the absorption spectrum of samples that dispersed in hydrochloric acid solution. The mean exciton absorption was found at Convergent values. The intensity of absorption is high, this is due to the high concentration of solution. The relation between the absorption and wavelength shows for the samples, and by using Tauc plot method the energy gap were calculated for Ca_2AlVO_6, Sr_2AlVO_6 and Ba_2AlVO_6, and found to be 4.16eV, 4.79eV and 4.87eV respectivily [22].

$$\alpha h\nu = A(h\nu - E_g)^n \qquad (3)$$

Where E_g the band gap, constant A is different for different transitions, (hv) is energy of photon and n value is respectively 1/2 and 2 for direct and indirect transition, Figure (7) refer to the Tauc plot of Ba_2AlVO_6 case, the wavelength and band gap energy were listed for the samples in table (3).

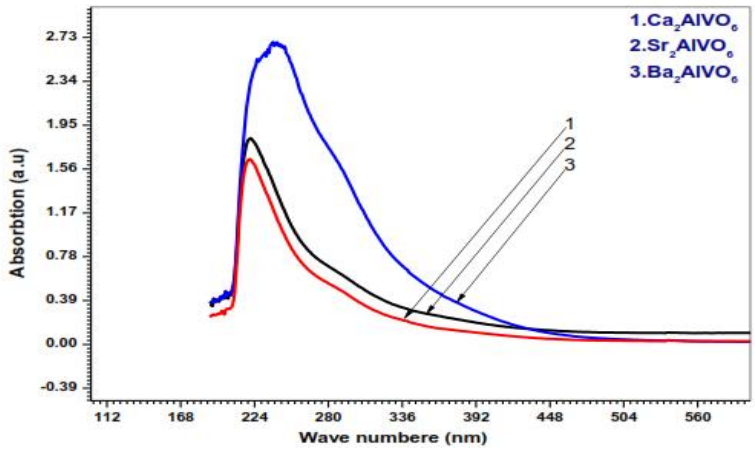

FIGURE 6: The UV.vis SPCTRUM Ca_2AlVO_6, Sr_2AlVO_6 and Ba_2AlVO_6 samples.

Impedance spectroscopy analysis

In order to understand the dynamics of the mobile ions (dielectric relaxtion) in X_2AlVO_6 where (X= Ca,Sr, and Ba), the complex plane impedance (z*=z`-z``)Plotes for X_2AlVO_6 where (X= Ca,Sr, and Ba) at room temperature are showen in fig.4 using cole cole plote. complex plane impedance spectra can be seen as semicircles Along frequencies and their center are depressed to below the real impedance axes, figure (8) express the complex plane impedance spectra Ba_2AlVO_6 case.

The samples have similar represented from relation between | Z | against the applied frequency. Figure (9) is graph of | Z | against the applied frequency shows that for Ba_2AlVO_6 case a higher values of | Z | with a long value of low frequency and vice-versa, that mean the dielectric constant was found at lower frequency and this refer to insulator behavior. The dielectric constant, impedance, resistivity and conductivity were calculated for all samples for X_2AlVO_6 where (X= Ca, Sr, and Ba) at room temperature, the positive dielectric constants might be attributed to insulator materials. Table (4) shows dielectric impedance parameters (and dielectric constant at ω = 100 Hz) at room temperature.

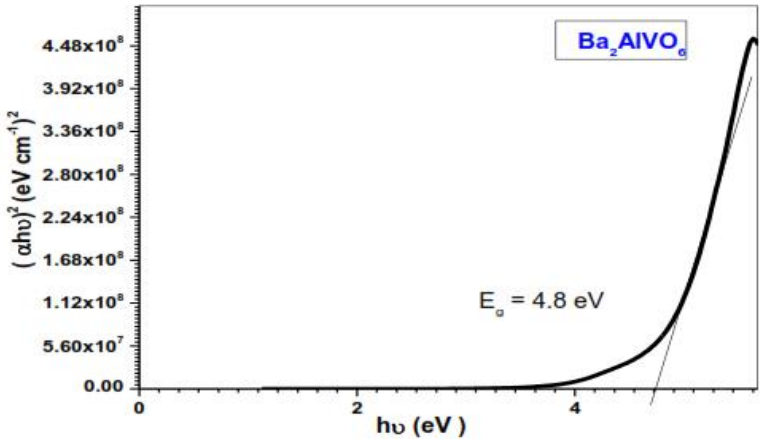

FIGURE 7: Give the plot of $(\alpha h\nu)^2$ in term of band gap for Ba_2AlVO_6 double perovskite

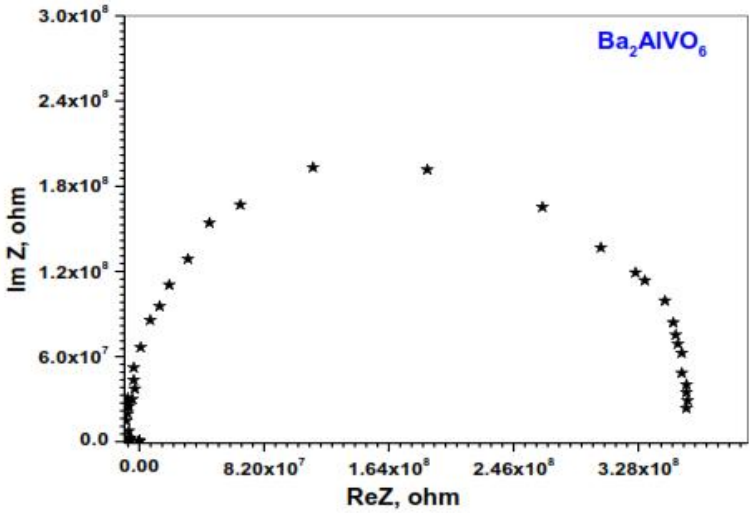

FIGURE 8: (Cole Cole plot) complex plane impedance spectra for Ba_2AlVO_6 sample

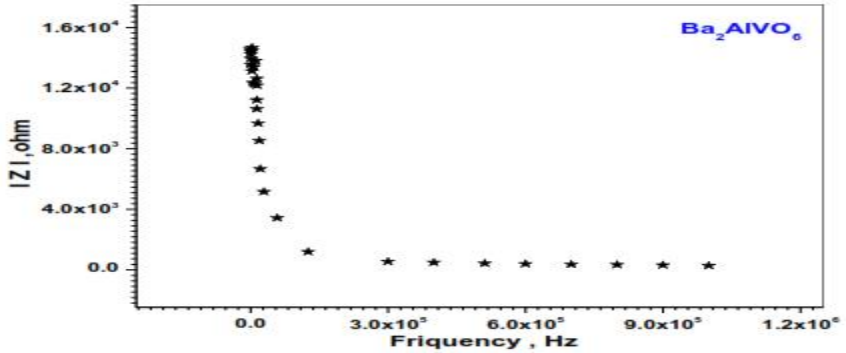

FIGURE 9: Graphs of |Z| against the applied frequency for Ba_2AlVO_6 sample.

CONCLUSION

The X-site substitutions of X_2AlVO_6 where (x = Ca, Sr and Ba) were achieved successfully using solid reaction method. XRD proved that the structure is orthorhombic with (pnma) space group and crystalline size was found to be 61.61, 69.83 and 76.38 nm. FTIR showed numbers of peaks and were assigned to double perovskite structure. UV studied and the energy band gap found to be in the range 4.1eV to 4.8 eV. Dielectric constants takes the positives values which are indicate that the samples possess an insulators behavior.

ACKNOWLEDGMENT

The authors would like to thank the physics department in college of science and technology Alneelain University particularly material lab for supporting this research. And also they thank Mr. Abdulsakhi for helping us in analysis of results.

REFERENCES

[1]. Perianu, E.A., Gorodea, I.A., Gheorghiu, F., Sandu, Av, Ianculescu Ac, Sandu I., REV CHIM (Bucharest). 2011; 62(1):17-20.

[2]. Kuzmanovski, I., Dimitrovska-Lazova, S., Aleksovska, S. Analytica Chimica Acta. 2007; 595 (1–2):182-9.

[3]. Galasso, F.S., Chapter 2 - Structure of Perovskite-type Compounds. In: Galasso FS, editor. Structure, Properties and Preparation of Perovskite-Type Compounds. 1969. Pergamon: p. 3-49.

[4]. Jeng, H-T., Guo, G.Y. Physical Review B. 2003; 67(9):094438.

[5]. Opel, M. Journal of Physics D: Applied Physics. 2012; 45(3):033001.

[6]. Peschel, S., Ziegler, B., Schwarten, M., Babel, D. Zeitschrift für anorganische und allgemeine Chemie. 2000; 626(7):1561-6.

[7]. Landínez Téllez, D.A., Martínez Buitrago, D., Cardona, C. R., Barrera, E.W., Roa-Rojas J. Journal of Molecular Structure. 2014;1067(0):205-9.

[8]. Elbadawi, A.A., Yassin, O.A., Gismelseed, A.A. Journal of Magnetism and Magnetic Materials. 2013;326(0):1-6.

[9]. Shaikh, M.W., Varshney, D. Materials Chemistry and Physics. 2012;134(2–3):886-98.

[10]. Sundarayya, Y., Mandal, P., Sundaresan, A., Rao, CNR. Journal of Physics: Condensed Matter. 2011;23(43):436001.

[11]. Bharti, C., Sinha, T.P. Physica B: Condensed Matter. 2012;407(1):84-9.

[12]. Zhou, X., Xiao, T., Zhao, X., Wang, Y., Li, L., Wang, Z. & Lee, Q. Journal of Luminescence. 2014;152(0):165-7.

[13]. Suryanarayana, C., Norton, M.G. X-Rays and Diffraction. X-Ray Diffraction. 1998. Springer US: p. 3-19.

[14]. Wu, Z-Y., Ma, C-B., Tang, X-G., Li, R., Liu, Q-X., Chen, B-T. Nanoscale Research Letters. 2013;8(1):207.

[15]. Kavitha, V.T., Jose, R., Ramakrishna, S., Wariar, P.R.S., Koshy, J. Bull Mater Sci. 2011;34(4):661-5.

[16]. Kim, H-S., Lee, C-R., Im J-H, Lee, K-B., Moehl, T., Marchioro, A., Moon, S.-J., Humphry-Baker, R., Yum, J.-H., Moser, J. E., Grätzel, M. & Park, N.-G. Scientific Reports. 2012; 2:591.

[17]. Yáñez-Vilar, S., Mun, E.D., Zapf, V.S., Ueland, B.G., Gardner, J.S., Thompson, J.D., Singleton, J., Sánchez-Andújar, M., Mira, J., Biskup, N., Señarís-Rodríguez, M. A. & Batista, C. D. Physical Review B. 2011;84(13):134427.

[18]. Bharti, C., Das, M.K., Sen, A., Chanda, S., Sinha, T.P. Journal of Solid State Chemistry. 2014; 210(1):219-23.

[19]. Salunkhe, A., Khot, V., Phadatare, M., Thorat, N., Joshi, R., Yadav, H. M. & Pawar, S. H. Journal of Magnetism and Magnetic Materials. 2014; 352:91-8.

[20]. Kim, Y-I., Woodward, P.M. Journal of Solid State Chemistry. 2007;180(10):2798-807.

[21]. Bharti, C., Sinha, T.P. Solid State Sciences. 2010;12(4):498-502.

[22]. Sánchez-Vergara, M.E., Alonso-Huitron, J.C., Rodriguez-Gómez, A., Reider-Burstin, J.N. Molecules. 2012;17(9):10000-13.